

Aperture variation and pressure change due to thermal stress and silica precipitation/dissolution accompanied by colloidal transport in a coupled fracture-skin-matrix system

N.Natarajan^{1*} and G. Suresh Kumar²

Abstract — A numerical model is developed for studying the fluid pressure and permeability changes in a coupled fracture matrix system in the presence of fracture-skin with colloidal transport in a fractured geothermal reservoir, by taking into account the effects of thermal stresses and silica precipitation/dissolution, which is computed using linear reaction kinetics. Thus, this work is essentially an extension of the earlier work by Ghassemi and Suresh Kumar (2007). In addition, in the present model, the contaminant transport is facilitated by the presence of colloids. Mass exchange between the horizontal fracture and the fracture-skin is accounted for by assuming diffusion limited transport for both colloids as well as contaminants. Heat transfer between the fracture and fracture-skin is modeled considering only conduction, while heat transport within the fracture includes thermal advection, dispersion and conduction. Due to colloid facilitated chemical transport under non isothermal conditions, in a coupled fracture-skin-matrix system, the fracture apertures vary spatially, with a corresponding pressure variation for a constant discharge. A series of numerical experiments were conducted for analyzing the spatial variation of fracture aperture in response to the individual and combined effects of thermal stress and silica precipitation/dissolution in the presence of the fracture-skin and colloids facilitated contaminant transport. Results suggest that the presence of fracture skin and colloids has a significant impact in deciding the evolution of fracture permeability.

Keywords— Fracture skin, Finite difference, Colloidal transport, Silica Precipitation/Dissolution.

¹Research Scholar, EWRE Division, Department of Civil Engineering, Indian Institute of Technology, Madras, Chennai-36, India. E-mail: itsrajan2002@yahoo.co.in

²Associate Professor, Department of Ocean Engineering, Indian Institute of Technology, Madras, Chennai – 36, India. E-mail: gskumar@iitm.ac.in

I. INTRODUCTION

Enhanced geothermal reservoir is a major source of renewable energy and the ultimate goal of geothermal reservoir development is to economically develop geothermal energy. The permeability of a Geothermal Reservoir is mainly dependent on the pre existing fractures and is affected by changes resulting from thermal, mechanical and chemical processes. The thermal energy stored in a rock is accessed by the fluid circulating between the injection and production well, which is subsequently used for the production of geothermal power. The movement of the geothermal fluid reacts with the adjacent rock-matrix leading to precipitation and dissolution of minerals due to the large gradient in temperature, pressure and concentration between the fracture and the rock-matrix. Many studies have been conducted by researchers on precipitation dissolution in geothermal reservoirs (Robinson 1982, Robinson and Pendergrass 1989, Cline et al. 1992, Malate and O'Sullivan 1992, Lowell 1993, Arvidson and Mackenzie 1999, Satman et al. 1999, Brien et al. 2003, Suresh Kumar and Ghassemi 2005, Ghassemi and Suresh Kumar, 2007, Taron et al. 2009, Taron and Elsworth 2009). While many researchers have studied about the precipitation dissolution in fractured media, only a few have focused on the fracture aperture variation. Ghassemi and Suresh Kumar (2007) analyzed the fracture aperture and pressure variation in a coupled fracture matrix system due to coupled precipitation-dissolution and thermoelastic stresses. The present work is an extension of the earlier study conducted by Ghassemi and Suresh Kumar (2007).

The previous studies have attempted investigations of precipitation and dissolution in the coupled fracture-matrix system. However, Sharp (1993) pointed out the possibility of the presence of fracture-skins in a fractured porous media. These are defined as low-permeability material deposited along the fracture walls. A few studies conducted with respect to solute transport in fracture-skins have concluded that

fracture-skins in the form of clay filling (Driese et al. 2001), mineral precipitation (Fu et al. 1994) and organic growth material (Robinson and Sharp 1997) have reduced the permeability in fracture-skin while some others have concluded that the presence of fracture-skins has increased the permeability in fracture-skins by developing micro-fractures (Polak et al. 2003). Analogous to solute transport, the presence of fracture-skin can significantly affect the heat conductivity in the fracture-matrix system. Natarajan and Suresh Kumar (2011) have numerically modeled thermal transport in the coupled fracture-matrix system in the presence of fracture-skin and analyzed the spatial moment of the thermal fronts with the aid of moment analysis. Their study concluded that the presence of fracture-skin can significantly affect the heat transfer mechanism between the fracture and rock-matrix in the geothermal reservoir. Natarajan and Suresh Kumar (2010a) have also analysed the effect of poroelastic and thermoelastic stresses in the coupled fracture-matrix system in the presence of fracture-skin and have concluded that the effect of poroelasticity is insignificant with respect to fracture aperture for low discharges. Thus, the effect of skin would have a significant impact on the precipitation dissolution mechanism and thermoelastic stresses in the coupled fracture-matrix system. Literature review also justifies the existence of colloids in a geothermal reservoir. For example, Hurtado et al. (1989) have reported the presence of colloidal silica in the geothermal system in Cerro Prieto Geothermal field. Potapov et al. (2002) have discussed the process for removing colloidal silica from geothermal brine in Mutnovskoe hydrothermal field (Kamchatka peninsula). Bourcier et al. (2003) have discussed the opportunities, processes, challenges and the economics of recovering minerals and metals from geothermal fluids. McLin et al. (2006) have reported the formation of colloidal silica precipitate in Coso and Salton Sea geothermal fields in California. The presence of colloids in the geothermal system would enhance the transport of contaminants in the subsurface media. Many studies have considered the presence of colloids in the transport of contaminants (Champ et al. 1982, Eichholz et al. 1982, Kretschmar et al. 1999). Significant research has been conducted on colloid facilitated contaminant transport in coupled fracture matrix system (Abdel-Salam and Chrysikopoulos 1994, Ibraki and Sudicky 1995, Baek and Pitt 1996, Chrysikopoulos and Abdel-Salam 1997, Abdel-Salam and Chrysikopoulos 1995). As far as transport of colloids in fracture-skin-matrix is concerned, Natarajan and Suresh Kumar (2010b) developed a numerical model for the colloid facilitated radionuclide transport in the coupled fracture-matrix system in the presence of fracture-skin. Their model assumed the radionuclides and colloids to decay as well as sorb on the fracture surface, diffuse into the fracture-skin and the rock-matrix. Filtration as well as remobilization of colloids was also considered in that model and sensitivity analysis was performed to investigate the effect of various colloid properties on the colloid concentration. Their study concluded that the presence of colloids hinders the diffusion of contaminants into the rock-matrix. Thus, the presence of colloids and formation of fracture-skin can significantly affect the efficiency of the geothermal reservoir, as they have direct

influence on the fracture permeability variation between the injection and production well, resulting from the aperture and pressure variation in the reservoir. As far as the author's knowledge is concerned, the previous studies have not addressed the combined effects of fluid flow (pressure variation), mass transport (colloid facilitated contaminant transport), non isothermal silica transport (reaction kinetics) and thermoelasticity in the coupled fracture-matrix system with fracture-skin with colloid facilitating the contaminant transport. The aim of this paper is to analyze the variation in fracture permeability and pressure due to the combined effect of the above processes. The effect of pH is assumed to be negligible.

II. PHYSICAL SYSTEM AND GOVERNING EQUATIONS

The conceptual model corresponding to a coupled fracture-skin-matrix system (Robinson et al. 1998) is illustrated in Fig.1.

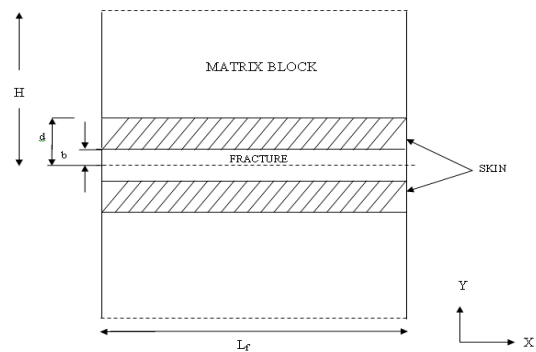


Fig. 1 Schematic diagram showing a coupled fracture-skin-matrix system

In Figure 1, b represents the half fracture aperture, $b-d$ represents the thickness of the fracture-skin and H represents the thickness of the half fracture spacing. The following assumptions are used in the present study:

1. The fracture aperture is much smaller in comparison with the length of the fracture.
2. Thermal dispersion is analogous to dispersion of solutes in fracture matrix system.
3. Convection within the fracture-skin and rock-matrix has been ignored by assuming that there is no fluid flow within the fracture-skin and rock-matrix.
4. Temperature at the fracture-skin interface, i.e., temperature along the fracture walls and along the lower boundary of the fracture-skin is assumed to be equal (at $y = b$).
5. Temperature at the skin-matrix interface, i.e., temperature along the upper boundary of the fracture-skin and the lower boundary of the rock-matrix is assumed to be equal (at $y = d$). The conductive flux in the fracture-skin is equal to the conductive flux in the rock-matrix at the skin-matrix interface as expressed in equation.

6. Specific heat capacities are not functions of temperature.
7. The solution is restricted to one half of the fracture and its adjacent fracture-skin and its associated rock-matrix by assuming symmetry.
8. Thermal conduction is considered both in the fracture, fracture-skin and the rock-matrix.
9. Only a single fluid phase exists.
10. Changes in fluid enthalpy with pressure are neglected.
11. Transverse diffusion and dispersion within the fracture assure complete mixing across the fracture thickness/aperture at all times.
12. Permeability of the fracture-skin and the rock-matrix is low, and molecular diffusion is assumed to be the main transport mechanism in them.
13. Transport along the fracture is much faster than transport in fracture-skin and the rock-matrix.
14. Fracture, fracture-skin and the rock-matrix are saturated.
15. Colloids are assumed to be unaffected by the thermal transport in the fracture and thus precipitation-dissolution is not considered for colloids.

The readers are advised to refer Suresh Kumar and Ghassemi (2005) for the governing equations of the flow module. The governing equations and the model assumptions for colloid facilitated contaminant transport have been adopted from Natarajan and Suresh Kumar (2010b) with radioactive decay term to be zero as the contaminants assumed in this model are not radionuclides. The governing equations for thermal transport in fracture-skin-matrix system have been adopted from Natarajan and Suresh Kumar (2011) to avoid repetition. The governing equations for precipitation and dissolution of quartz in the coupled fracture-skin-matrix system are described below.

Precipitation dissolution of quartz in the fracture-skin-matrix system

The principal solute transport mechanisms in the fracture are advection, describing the motion of dissolved particles along the circulating fluid, free molecular diffusion within the fracture in the direction of fracture axis, diffusion limited solute transport at the fracture-skin interface, dissolution of quartz within the fracture and effective diffusion within the fracture-skin. The coupling between the fracture and skin is ensured by the continuity of the fluxes between them by assuming that the conductive flux from the fracture to the skin takes place in a direction perpendicular to the fracture. The quartz dissolution is described by linear reaction kinetics and the modified form of fracture, fracture-skin and matrix equations are given by (Steeffel and Litchner 1998):

$$\frac{\partial S}{\partial t} = v_f \frac{\partial S}{\partial x^2} - k_f S + \frac{\theta_p D_p}{b} \frac{\partial S_p}{\partial y} \Big|_{y=b} \quad (1)$$

$$\frac{\partial S_p}{\partial t} = D_p \frac{\partial^2 S_p}{\partial y^2} - \frac{k_p}{\theta_p} S_p \quad (2)$$

$$\frac{\partial S_{mat}}{\partial t} = D_{mat} \frac{\partial^2 S_{mat}}{\partial y^2} - \frac{k_{mat}}{\theta_{mat}} S_{mat} \quad (3)$$

Where k , k_p , k_{mat} refers to the rate constant in the fracture, fracture-skin and in the rock-matrix, which are dependent on temperature. The quartz concentration in the fracture, fracture-skin and rock-matrix can be obtained using the expressions given below:

$$S' = S - S^{eq} \quad (4)$$

$$S_p' = S_p - S_p^{eq} \quad (5)$$

$$S_{mat}' = S_{mat} - S_{mat}^{eq} \quad (6)$$

where S is the total dissolved concentration in the fracture, S_p is the total dissolved concentration in the fracture-skin and S_{mat} is the total dissolved concentration in the rock-matrix. S^{eq} , S_p^{eq} and S_{mat}^{eq} are the equilibrium concentration in fracture, fracture-skin and matrix which are temperature dependent.

The initial and boundary conditions associated with equations (4)-(6) are as follows:

$$S(x, t = 0) = S_p(x, y, t = 0) = S_{mat}(x, y, t = 0) = 0 \quad (7)$$

$$S(x = 0, t) = S_o \quad (8)$$

$$S(x = L_f, t) = 0 \quad (9)$$

$$S(x, t) = S_p(x, y = b, t) \quad (10)$$

$$\theta_p D_p \frac{\partial S_p(x, y = d, t)}{\partial y} = \theta_{mat} D_{mat} \frac{\partial S_{mat}(x, y = d, t)}{\partial y} \quad (11)$$

$$S_p(x, y = d, t) = S_{mat}(x, y = d, t) \quad (12)$$

$$\frac{\partial S_{mat}(x, y = H, t)}{\partial y} = 0 \quad (13)$$

The temperature dependent equilibrium concentration adopted by Pendergrass and Robinson (1989) from Rimstidt and Barnes (1980) is

$$S^{eq} = 6 * 10^4 * 10^{(1.881 - 2.028 * 10^{-3} T - 1560/T)} \quad (14)$$

where equilibrium concentration is in ppm and temperature is in K.

The temperature dependent dissolution rate constant is given by (Robinson 1982)

$$k = 10^{(0.433 - 4090/T)} \quad (15)$$

where the units of k are m/s.

In order to compute the mass of silica deposited along in the fracture at various times, the cumulative mass of silica dissolved along the fracture is examined using the approach followed by Robinson and Pendergrass (1989). For each time interval, the mass of silica dissolved per unit fracture length is given by

$$m_q = \frac{10^{-6} \rho_w \Delta t V_f k a^* (S^{eq} - S)}{L_f} \quad (16)$$

where ρ_w is the density of the circulating fluid in the fracture, $V_f (= A_f L_f)$ is the volume of fluid in the fracture, L_f is the length of the fracture and $A_f (= 2b \cdot 1)$ is the cross-sectional area of the fracture perpendicular to the flow direction. Since the fluid flow occurs in the fractures, a relationship is developed for a^* assuming that the fracture can be approximated by the parallel plate model:

$$a^* = \frac{2f_q}{2b} \quad (17)$$

where f_q is the volume fraction of quartz in the rock-matrix and $2b$ is the mean fracture aperture. The quantity of silica dissolved in the fracture is related to the fractional aperture change in the average fracture aperture by assuming the fracture flow geometry (Robinson and Pendergrass, 1989). For each time step, the fractional aperture change, Δw , resulting from the chemical interaction between the fracture and rock-matrix is related to the function of total rock-matrix volume and its components and is given as (Robinson and Pendergrass 1989).

$$\Delta w = \frac{-L_f m_q}{\rho_q V_f} \quad (18)$$

where ρ_q is the density of quartz, V_f is the fluid volume in the fracture, L_f is the length of the fracture.

Fracture aperture change due to thermo elasticity

The expression for rock displacement as a function of temperature is given by Ghassemi and Suresh Kumar (2007) has been modified.

$$\frac{\partial u_y}{\partial t} = \frac{1}{2} \frac{\partial w(x,t)}{\partial t} = \frac{(1+\nu)\alpha_T \lambda_s}{(1-\nu)\rho_s C_s} \frac{\partial \Delta T(x,y,t)}{\partial y} \Big|_{y=0} \quad (19)$$

where ν is the Poisson's ratio and α_T is the linear thermal expansion coefficient.

The analytical solution for heat flux at the interface of the fracture and rock-matrix given by Bodvarsson (1969) has been modified to account for the fracture-skin.

$$\frac{T_{s0} - T(x,y,t)}{T_{s0} - T_{f0}} = \operatorname{erfc} \left[\frac{\sqrt{\lambda_s \rho_s C_s}}{QC_w \rho_w \sqrt{t}} x + \sqrt{\frac{\rho_s C_s}{\lambda_s t}} \frac{y}{2} \right] \quad (20)$$

Where T_{s0} is the initial fracture-skin temperature, T_{f0} is the initial injection fluid temperature, Q the volumetric injection rate, ρ_w the fluid density and C_w is the water specific heat. If we assume the temperature at infinity is T_{s0} and $\Delta T = T_{s0} - T_{f0}$, we can write eq.(20) as :

$$T(x,y,t) - T_{s0} = -\Delta T \operatorname{erfc} \left[\frac{x\sqrt{\lambda_s \rho_s C_s}}{QC_w \rho_w \sqrt{t}} + \sqrt{\frac{\rho_s C_s}{\lambda_s t}} \frac{y}{2} \right]$$

or $T(x,y,t) - T_{s0} = -\Delta T \operatorname{erfc}(A_1 + A_2 y)$ where

$$A_1 = \frac{x\sqrt{\lambda_s \rho_s C_s}}{QC_w \rho_w \sqrt{t}} \quad \text{and} \quad A_2 = \sqrt{\frac{\rho_s C_s}{\lambda_s t}} \frac{1}{2}$$

Differentiating eq.(20) with respect to y :

$$\frac{\partial T(x,y,t)}{\partial y} \Big|_{y=0} = \frac{2\Delta T A_2}{\sqrt{\pi}} \exp[-(A_1 + A_2 y)^2] = \frac{2\Delta T A_2}{\sqrt{\pi}} \exp[-(A_1)^2] \quad (21)$$

Substituting eq.(21) into eq.(19) yields:

$$\frac{\partial w(x,t)}{\partial t} = \frac{2(1+\nu)\alpha_T \lambda_s}{(1-\nu)\rho_s C_s} \left(\frac{2\Delta T A_2}{\sqrt{\pi}} \exp[-(A_1)^2] \right) \quad (22)$$

III. NUMERICAL MODEL

In this study, the system is described by a set of three partial differential equations, one equation for the fracture, one for the fracture-skin and the remaining for the rock-matrix, formulated for a one-dimensional framework. The system of equations is non linear and couples the fracture, fracture-skin and the rock-matrix. The coupled system is solved numerically using implicit finite difference scheme. The continuity at the fracture-skin interface is attained by iterating the solution at each time step. This is carried out in solving both colloid facilitating contaminant transport as well as the thermal transport. A non uniform grid is adopted in the fracture-skin and rock-matrix. A smaller grid size is adopted in the fracture-skin interface to accurately capture the flux transfer at the fracture-skin interface.

Initially, the colloid facilitated contaminant concentration is obtained by solving the governing equations pertaining to colloid facilitated contaminant transport in a coupled fracture-skin-matrix system. The temperature distribution along the fracture in the coupled system is obtained by solving the governing equations for thermal transport in the domain. Having found the temperature distribution, the thermoelastic changes in fracture aperture are calculated using the analytical solution provided in equation (22) and the new fracture aperture is computed. The computed temperature distribution is then used to calculate the reaction constants for the fracture, fracture-skin and the rock-matrix using equation (15) and thus evaluate the new equilibrium concentration of silica using equation (14). The reaction constants along with the existing contaminant concentration are used to calculate the total

dissolved concentration using equations (1), (2) and (3). This concentration is finally used in computing the quartz concentration in the fracture, fracture-skin and rock-matrix using equations (4), (5) and (6). Based on this quartz concentration, the mass of silica deposited/dissolved is computed using equation (16) and the aperture change is calculated using expression (18). The new fracture aperture is obtained by adding this with the previous value. The final updated fracture aperture is used to calculate the pressure variation using the Cubic law. The old values of temperature and concentration profiles are updated for the next time step. An iteration process is carried out as shown below between the fracture and fracture-skin temperatures and concentrations at the fracture and skin interface. The coupling between the various components described above has been shown using a flow chart in Figure 2.

The discretisation of the coupling term representing the last term in equation (1) indicates the coupling at the interface of the fracture and the fracture-skin. This coupling is discretised as

$$\frac{\partial S_p}{\partial t} = \frac{S_{p2}^{n+1} - S_{p1}^{n+1}}{\Delta y(1)}$$

The concentration in the first node of the fracture-skin becomes equal to the fracture concentration at the interface of the fracture and the fracture-skin satisfying the assumed boundary condition, i.e.

$$S_{p1}^{n+1} = S^{n+1}$$

Since the concentration of the second node in the fracture-skin (S_{p2}^{n+1}) is known only at the initial time ($t = 0$) and is unknown at the next time step, i.e. $(n+1)^{\text{th}}$, the value is assumed and iterated until convergence is achieved. Thus the concentrations for the i^{th} , $(i-1)^{\text{th}}$ and $(i+1)^{\text{th}}$ nodes are solved at the next time step, i.e. $(n+1)^{\text{th}}$ and the fourth unknown in the equation (S_{p2}^{n+1}) is assumed and iterated until convergence is achieved.

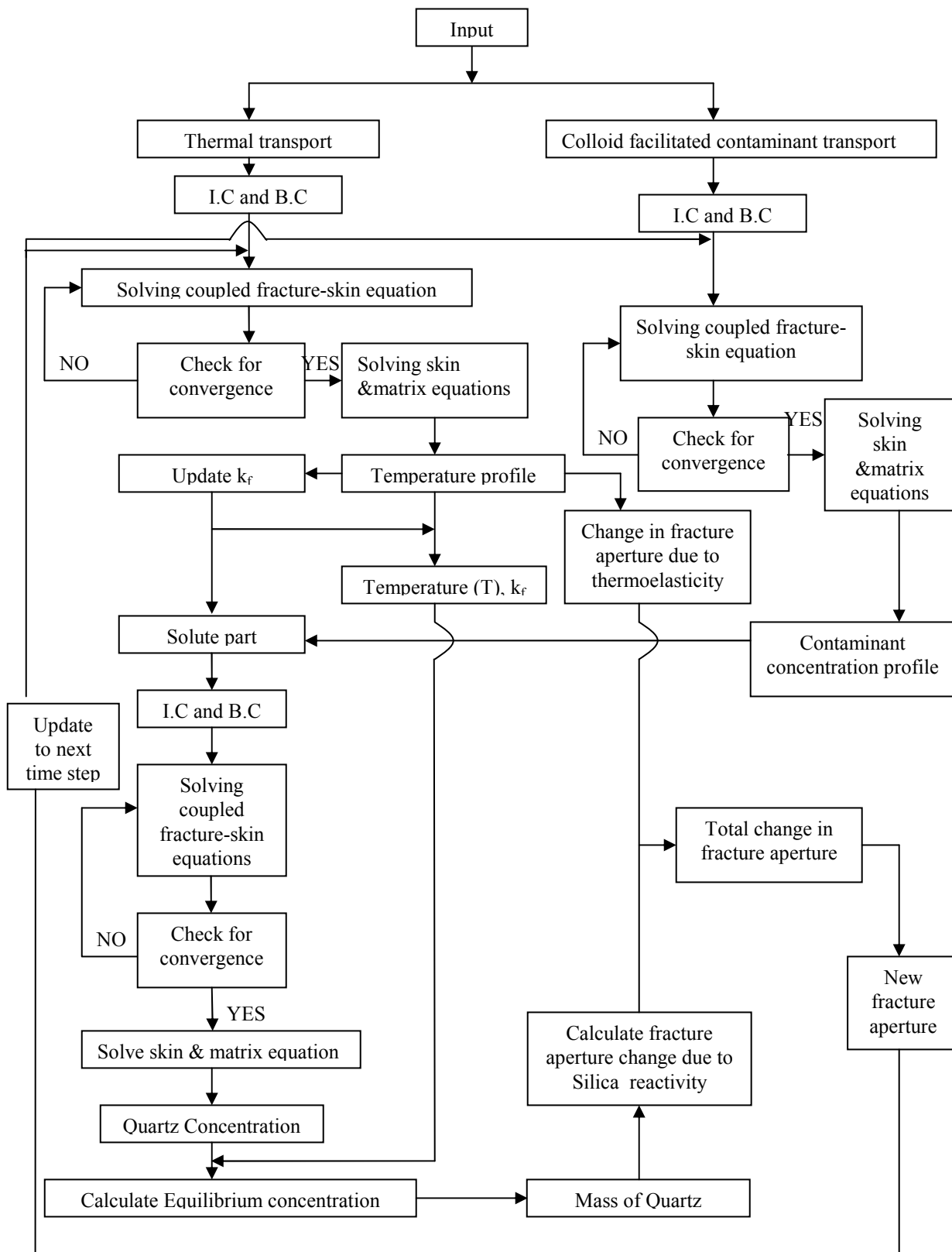


Fig. 2 Coupling of contaminant transport, heat transport and reactive solute transport in a coupled fracture-skin-matrix system

IV. RESULTS AND DISCUSSION

An implicit finite difference numerical model is developed to determine the evolution of fracture permeability and fluid pressure resulting from precipitation/dissolution of quartz in the presence of fracture-skin and colloid facilitated contaminant transport. The study considers situations in which the water entering the fracture, either supersaturated or undersaturated with respect to quartz flows through the fracture-skin-matrix system. As the water entering the fracture gets heated by conduction, cools the rock, leading to thermal stresses in the rock mass and changes the silica concentration in the fracture.

A scaled/relative concentration can be any concentration that is conserved in a chemical Reaction (Ghassemi and Suresh Kumar 2007). The equilibrium concentration obtained from Rimstidt and Barnes (1980), in terms of parts per million, is converted into millimoles/litre (mM /L) by dividing by the molecular weight of silica (60.08 g /mol). Depending on the nature of the injected fluid, the contaminant concentration at the inlet of the fracture (or injection well) may be maintained either at undersaturated or oversaturated concentration. A scaled or relative concentration of 1.0 is used as the boundary condition at the injection well, so that the constant relative contaminant concentration at the fracture inlet could be 0.25 (25mM/L) or 0.02 (2mM/L) when the injection fluid is oversaturated or undersaturated with respect to quartz, respectively (Ghassemi and Suresh Kumar 2007). The equilibrium concentration value for quartz is 10mM/L.

The dataset that was adopted by Natarajan and Suresh Kumar (2010b) in simulating colloid facilitated contaminant transport in fracture-skin-matrix system has been adopted for this study also. The parameters are provided in Table 1. The dataset used for thermal transport in fracture-skin-matrix system is given in Table 2.

Table 1 Parameters used for the colloid facilitated contaminant transport

Parameter	Symbol	Value
Initial half-fracture aperture (m)	b	200e-06
Fracture-skin thickness (m)	d-b	0.02
Fracture spacing (m)	2H	0.2
Diffusion coefficient of contaminants within the fracture-skin (m ² /year)	D _p	0.01
Diffusion coefficient of contaminants within the rock-matrix (m ² /year)	D _{mat}	0.01
Porosity of the fracture-skin	θ	0.09
Distribution coefficient for	K_{d_N}	0

contaminants on the fracture surface (m)		
Distribution coefficient for contaminants in fracture-skin (m)	$K_{d_{NP}}$	0
Distribution coefficient for contaminants in rock-matrix (m)	$K_{d_{Nmat}}$	0
Hydrodynamic dispersion coefficient of contaminants dissolved in the fracture aqueous phase (m ² /year)	D	10
Distribution coefficient for contaminants with mobile colloids within the fracture (for colloid diameter of 300nm) (m ³ /kg)	K_{d_m}	40
Distribution coefficient for contaminants with immobile colloids within the fracture (m ³ /kg)	$K_{d_{im}}$	40
Distribution coefficient for contaminants with mobile colloids within the fracture-skin (m ³ /kg)	$K_{d_{mP}}$	40
Distribution coefficient for contaminants with immobile colloids within the fracture-skin (m ³ /kg)	$K_{d_{imP}}$	40
Distribution coefficient for contaminants with mobile colloids within the rock-matrix (m ³ /kg)	$K_{d_{mmat}}$	40
Distribution coefficient for contaminants with immobile colloids within the rock-matrix (m ³ /kg)	$K_{d_{immat}}$	40
Average velocity of colloids in the fracture (m/year)	V _c	1
Colloid concentration at the inlet of the fracture (kg/m ³)	C _o	1
Hydrodynamic dispersion coefficient of colloids suspended in the rock fracture (m ² /year)	D _c	1
Filtration coefficient for colloids (m ⁻¹)	λ_f	0.5
Percentage of diffusion for colloids	ε	0.5

Diffusion coefficient of colloids within the fracture-skin (m^2/year)	D_{CP}	2.2e-08
Diffusion coefficient of colloids within the rock-matrix (m^2/year)	D_{Cmat}	1.5e-09
Distribution coefficient for colloids within the fracture-skin	$K_{d_{CP}}$	0.1
Distribution coefficient for colloids within the rock-matrix	$K_{d_{Cmat}}$	0.01
Remobilisation coefficient for colloids in the fracture (year^{-1})	Rmb	0.5
Length of the fracture (m)	L	50
Total simulation time (year)	T	5
Concentration of contaminants at the inlet of the fracture (kg/m^3)	N_o	1

Table II Parameters used for thermal transport in fracture-skin-matrix system

Parameter	Symbol	Value
Initial fracture aperture (μm)	b	200
Thermal dispersivity (m)	β_T	0.05
Rock-matrix specific heat capacity	C_m	800
Rock density (Kg/m^3)	ρ_m	2600
Thermal conductivity of the rock-	λ_m	2
Specific heat capacity of the fracture-skin ($\text{J}/\text{Kg}/\text{K}$)	C_s	1500
Fracture-skin density (Kg/m^3)	ρ_s	1500
Thermal conductivity of the fracture-	λ_s	2
Rock-matrix porosity	θ	0.05
Specific heat capacity of fracture	C_f	5000
Fracture fluid density (Kg/m^3)	ρ_f	1000
Thermal conductivity of fracture fluid	λ_f	0.5
Initial temperature (matrix and	T_0	600
Temperature at the inlet of the	T_i	300
Length of the fracture (m)	L	50
Total simulation time (year)	T	5
Poisson's ratio	ν	0.25
Linear thermal expansion coefficient	α_T	8e-06
Volume fraction of quartz in rock-		0.2

In this section, the results obtained from the chemical component of the model alone is discussed first followed by the results obtained from the combined effects of chemical and thermoelastic effects for both supersaturated and undersaturated fluid.

Role of silica precipitation and dissolution

Silica precipitation results in deposition of silica on the fracture aperture wall surface and silica dissolution results in loss of silica from the fracture surface. The dissolution or precipitation of silica also depends on whether the injected water is undersaturated or supersaturated. The injected cold water picks up heat from the rock-matrix which is further enhanced by the presence of fracture-skin which heats up the water as it moves along the fracture.

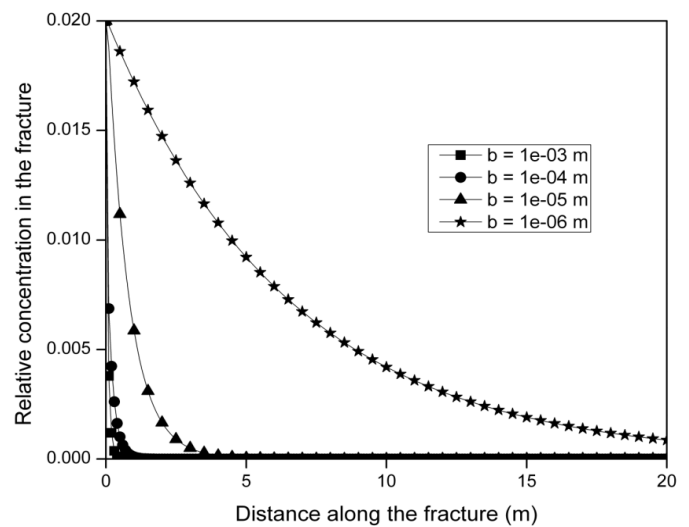


Fig. 3 Spatial distribution of relative concentration of contaminants along the fracture for various initial half fracture apertures. Flow rate = $5 \times 10^{-4} \text{ m}^3/\text{year}$. Fluid entering the fracture is under saturated (100 ppm). Refer Table 1 and 2 for other data.

Figure 3 represents the spatial distribution of relative concentration of contaminants along the fracture for various initial half fracture apertures. The incoming fluid is assumed to be under-saturated and a constant flow rate is assumed in the fracture. As colloids are also getting transported along with the contaminants, the contaminants get sorbed on the surface of the colloids due to their large surface area. This hinders the migration of contaminants along the fracture. Hesham et al. (2006) and Ren and Packman (2004) have concluded that the colloids can reduce the mobility of contaminants in the subsurface media. It is observed from Figure 3 that the concentration of contaminants increases in the fracture with reduction in half fracture aperture, unlike the usual observation where the contaminant concentration in the fracture reduces with reduction in fracture aperture due to significant matrix diffusion. This is because of the filtration of colloids from the

aqueous phase, which increases with reduction in fracture aperture. This reduces the diffusion of colloids and contaminants into the fracture-skin. Moreover, the velocity of the fluid increases with reduction in fracture aperture since a constant flow rate has been assumed. For very low fracture apertures, velocity of the fluid is high and thus the residence time available for the contaminants to diffuse into the fracture-skin is very low, resulting in high concentration of contaminants within the fracture.

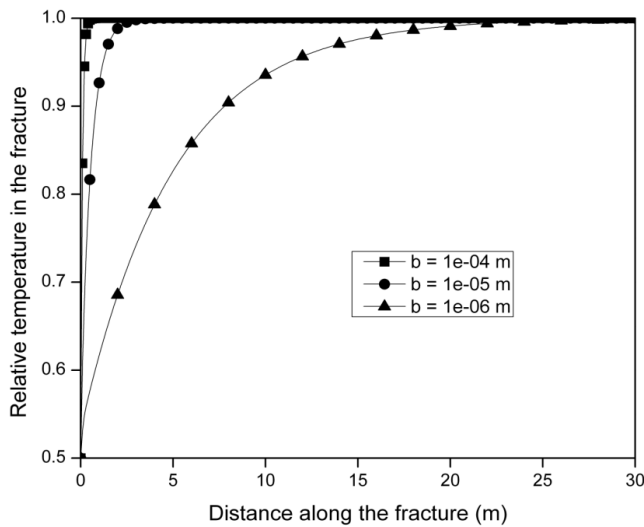


Fig. 4 Spatial distribution of relative temperature along the fracture for various initial half fracture apertures, Flow rate = 5×10^{-4} m³/year. Fluid entering the fracture is under saturated (100 ppm). Refer Table 1 and 2 for other data.

Figure 4 illustrates the spatial distribution of temperature along the fracture for various initial half fracture apertures. The injected fluid is assumed to be under-saturated and constant flow rate is assumed along the fracture. The rate of heat transfer increases with reduction in half fracture aperture in the presence of fracture-skin, according to the conclusion of Natarajan and Suresh Kumar (2011). From figure 4, it can be observed that as the half fracture aperture is reduced, the relative temperature in the fracture takes a longer time to attain the rock-matrix temperature. This is because, as the fracture aperture is reduced, the velocity of the fluid increases. This reduces the residence time for the fluid to extract heat from the fracture-skin and thus matrix temperature is attained far away from the fracture inlet even in the presence of fracture-skin.

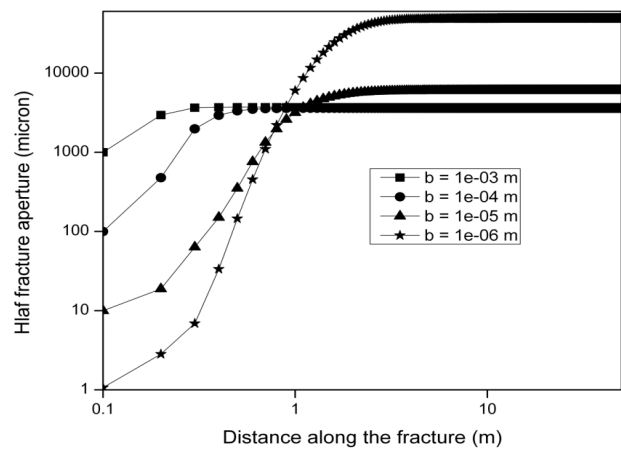


Fig. 5 Variation of half fracture aperture along the fracture for various initial half fracture apertures ($t = 5$ years, Flow rate = 5×10^{-4} m³/year, fluid entering the fracture is under-saturated (100ppm), Refer Table 1 and 2 for other data)

Figure 5 represents the variation of half fracture aperture along the fracture for various initial half fracture apertures. The fluid entering the fracture is assumed to be under saturated. It is observed from the figure that when the initial half fracture aperture is very high ($b_0 = 1 \times 10^{-3}$ m), the variation in the half fracture aperture is marginal near the injection well but remains constant thereafter. This is because of the rapid heat transfer taking place between the fracture-skin and the fracture as observed in Figure 4. This reduces the rate of silica reactivity along the fracture. On the other hand, for low initial fracture aperture ($b_0 = 1 \times 10^{-6}$ m), the half fracture aperture increases by four orders of magnitude near the injection well. This is because gradual increment in the temperature along the fracture (Fig.4) and high concentration of contaminants in the fracture (Fig.3), which increases the effect of silica reactivity along the fracture and thus the fracture variation is observed upto 5 m from the injection well. The portion of the fracture, subjected to aperture variation, increases with reduction in initial fracture aperture.

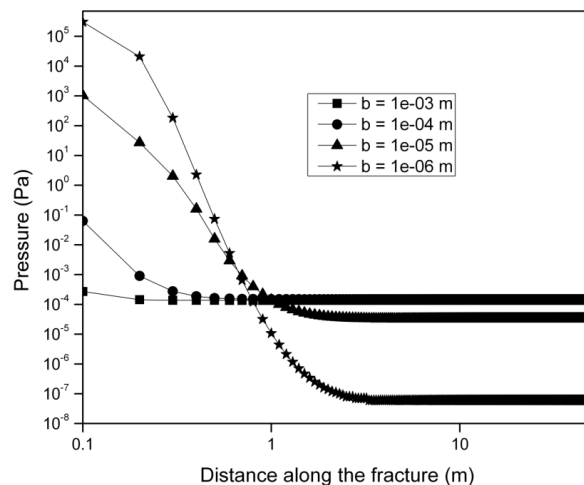


Fig. 6 Variation of pressure along the fracture for various initial half fracture apertures ($t = 5$ years, Flow rate = 5×10^{-4} $m^3/year$, fluid entering the fracture is under-saturated (100ppm), Refer Table 1 and 2 for other data)

Figure 6 shows the pressure variation along the fracture for various initial half fracture apertures. It is observed from Figure 6 that the pressure drop is very low near the injection well for large initial fracture apertures as the fracture variation is also low (Figure3). On the other hand, for very low initial fracture apertures, pressure drops by several orders of magnitude near the injection well as the half fracture aperture also varies significantly along the fracture.

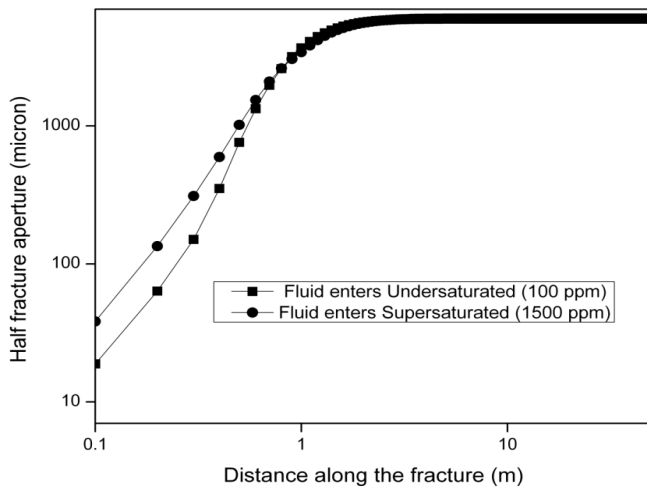


Fig. 7 Variation in half fracture aperture along the fracture when under and super saturated fluid is entering into the fracture ($t = 5$ years, initial fracture aperture $b_0 = 1 \times 10^{-5}$ m, Flow rate = 5×10^{-4} $m^3/year$). Refer Table 1 and 2 for other data.

Figure 7 provides the variation of half fracture aperture along the fracture for under and super saturated fluid entering the fracture aperture. A flow rate of 5×10^{-4} $m^3/year$ and an initial fracture aperture of 1×10^{-5} m were assumed for this simulation. Ghassemi and Suresh Kumar (2007) have observed that the under saturated entering fluid caused dissolution of silica from the fracture aperture while super saturation causes both dissolution as well as precipitation. It is observed from here from Figure 7 that both the under saturated fluid and super saturated fluid has caused dissolution of fracture aperture. This is because of the sorption of contaminants on the colloids within the aqueous medium and also on those colloids sorbed on the fracture wall surface. Consequently, the intensity of silica reactivity is increased resulting in dissolution of silica from the fracture surface. Additionally, the colloids sorbed on the fracture wall surface hinder the deposition of silica on the surface of the fracture walls in the case of super saturated fluid. As a result, dissolution is observed in both under saturated and super saturated cases. The nature of fracture

aperture variation near to the injection well differs for both the cases but a constant fracture aperture is attained after 1m from the fracture inlet.

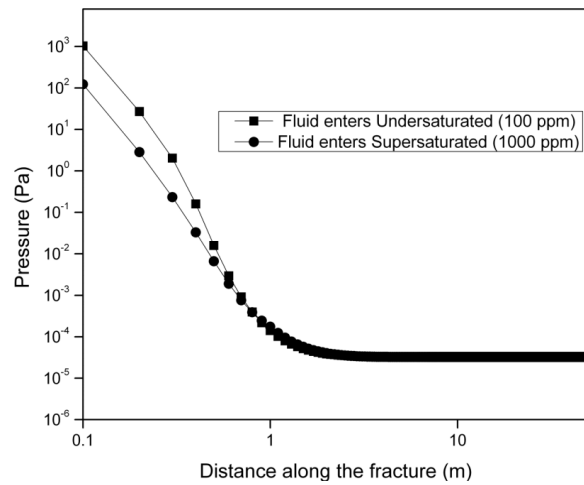


Fig. 8 Variation in pressure along the fracture when under and super saturated fluid is entering into the fracture ($t = 5$ years, initial fracture aperture $b_0 = 1 \times 10^{-5}$ m, Flow rate = 5×10^{-4} $m^3/year$). Refer Table 1 and 2 for other data.

Figure 8 provides the variation of pressure along the fracture for under and super saturated fluid entering the fracture aperture. A flow rate of 5×10^{-4} $m^3/year$ and an initial fracture aperture of 1×10^{-5} m were assumed for this simulation. It is observed from Figure 8 that the pressure drops along the fracture for both the under saturated and super saturated cases corresponding to the half fracture aperture variation for both the cases observed in Figure 7. The pressure at the inlet of the fracture is higher by an order of magnitude for the undersaturated condition compared to the case where the fluid enters the fracture in supersaturated condition.

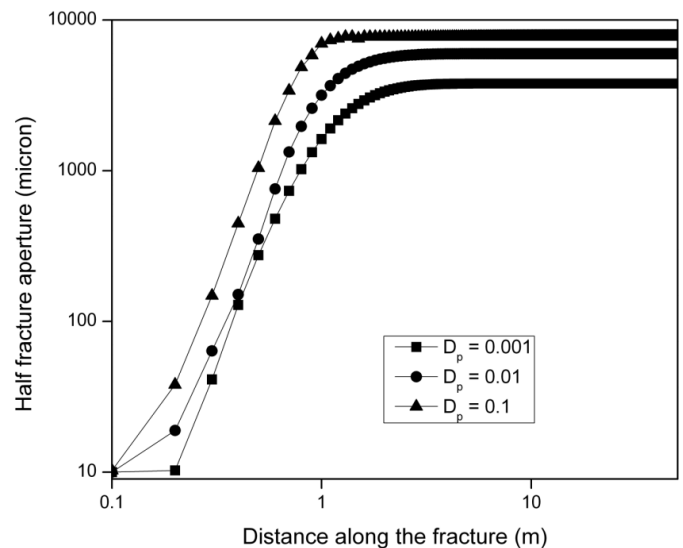


Fig. 9 Variation of half fracture aperture along the fracture for various fracture-skin diffusion coefficients ($t = 5$ years, Flow rate = $5e-04$ m³/year, $b_0 = 1 \times 10^{-5}$ m, fluid entering the fracture is under-saturated (100ppm). Refer Table 1 and 2 for other data)

Figure 9 shows the variation of half fracture aperture along the fracture for various skin diffusion coefficients. It is observed from Figure 9 that the half fracture aperture variation increases with increase in fracture-skin porosity. Ghassemi and Suresh Kumar (2007) have reported that the half fracture aperture variation decreases with increase in rock-matrix porosity. As the skin porosity increases, it enhances the filtration of colloids on the fracture surface. The filtered colloids on the fracture surface hinder further diffusion of contaminants and colloids into the fracture-skin which increases the concentration of contaminants within the fracture. This aggravates the silica reactivity and consequently the half fracture variation increases with increment of skin porosity. Moreover, the remobilization of colloids also contributes the high concentration of contaminants in the fracture.

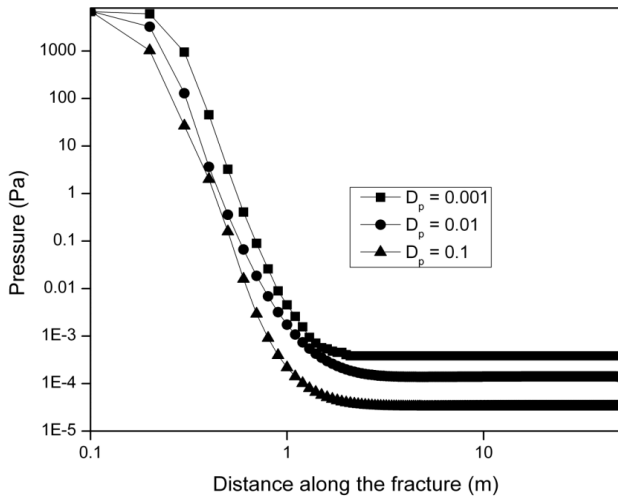


Fig. 10 Variation of pressure along the fracture for various fracture-skin diffusion coefficients ($t = 5$ years, Flow rate = 5×10^{-4} m³/year, $b_0 = 1 \times 10^{-5}$ m, fluid entering the fracture is under-saturated (100ppm). Refer Table 1 and 2 for other data)

Figure 10 shows the pressure variation along the fracture for various fracture-skin diffusion coefficients. The pressure near the injection well is the same for the all the cases but reduces along the fracture and attains a constant value after 1m from the fracture inlet. Pressure variation in the fracture is very high when the fracture-skin porosity is very high nearer to the injection well and the converse is observed when the fracture-skin porosity is very low. The pressure variation corresponds to the fracture aperture variation along the fracture.

Role of thermoelastic stresses

The effect of thermoelastic stresses on the fracture aperture has been analysed for various fluid velocities within the fracture.

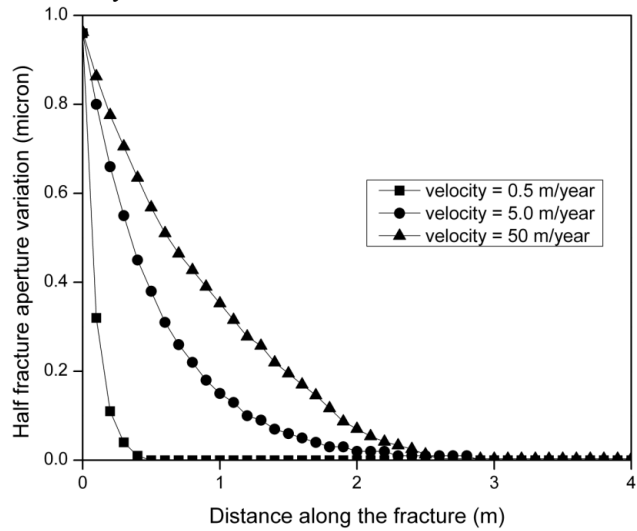


Fig.11 Change in the fracture aperture due to thermoelastic stresses for various fluid velocities. ($t = 5$ years, Flow rate = 5×10^{-4} m³/year, fluid entering the fracture is under-saturated (100ppm). Refer Table 1 and 2 for other data)

Fig.11 provides the spatial variation of fracture aperture due to thermoelastic stress for various fluid velocities. The effect of thermal stresses on fracture aperture in the fracture-skin-matrix system is analysed by neglecting the influence of silica dissolution. As observed from the figure, the stresses significantly change the fracture apertures near the inlet of the fracture and the impact diminishes with distance from the inlet. A small variation in the fracture aperture can significantly affect the flow along the fracture and thus it is important to consider the effect of thermoelastic stresses on the fracture aperture. When the velocity is low, there is significant residence time for the fluid in the fracture which enhances the thermal diffusion from the rock-matrix to the fracture through the medium of fracture-skin and thus fracture aperture variation is observed very close to the injection well compared to other cases with high fluid velocity.

Role of combined thermoelastic and chemical effects for undersaturated fluid injection

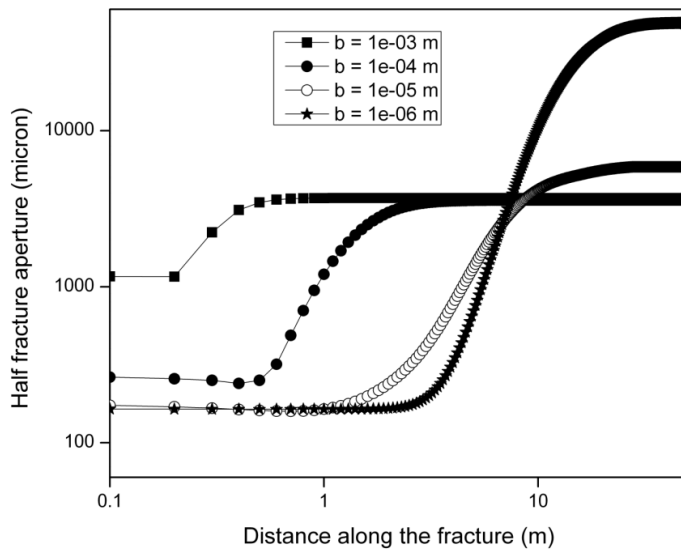


Fig. 12 Variation of half fracture aperture along the fracture for various initial half fracture apertures under the combined effects of thermoelastic stresses and chemical effects ($t = 5$ years, Flow rate = $5e-04$ $m^3/year$, fluid entering the fracture is under-saturated (100ppm), Refer Table 1 and 2 for other data)

Figure 12 represents the variation of half fracture aperture along the fracture for various initial half fracture apertures. The fluid entering the fracture is assumed to be under saturated and the analysis has been performed under the combined effects of thermoelastic stresses (thermal effect) and silica reactivity (chemical effect). For an initial fracture aperture of 1000 microns, the effect on the fracture aperture due to thermoelastic stresses is very less near the fracture inlet and after a short distance from the injection well the effect of silica reactivity is observed. The pattern of fracture aperture change due to the chemical reaction is the same as that observed in Figure 5 for the fracture aperture $b_0 = 1 \times 10^{-3} m$. For an initial fracture aperture of 100 microns, the effect of thermoelastic stresses is very high near the injection well due to the effect of the fracture-skin as the fracture aperture has risen upto 500 microns (approximately) and then the effect of silica reactivity is observed as the fracture aperture further rises and attains a constant value same as that attained with $b_0 = 1 \times 10^{-3} m$. The fracture aperture remains constant after a short distance because the filtered and remobilized colloids hinder the heat transfer mechanism at the interface of the fracture and the skin. This suppresses the effect on silica reactivity and thermoelastic stresses. For an initial fracture aperture of 10 microns, the effect of thermoelastic stresses is very high at the inlet of the fracture and remains constant for a considerable distance from the injection well. Then the fracture aperture increases by an order of magnitude due to the combined effects of thermoelastic stresses and silica reactions. This is because of the increment in fluid velocity due to reduction in fracture aperture which leads to gradual increment in temperature along

the fracture. For the case where the initial fracture aperture is very low ($b_0 = 1 \times 10^{-6} m$), the fracture aperture variation close to the fracture inlet is similar to the previous case but as time progresses the fracture aperture increases by more than two orders of magnitude due to the combined effect of thermoelastic stresses and chemical reactions.

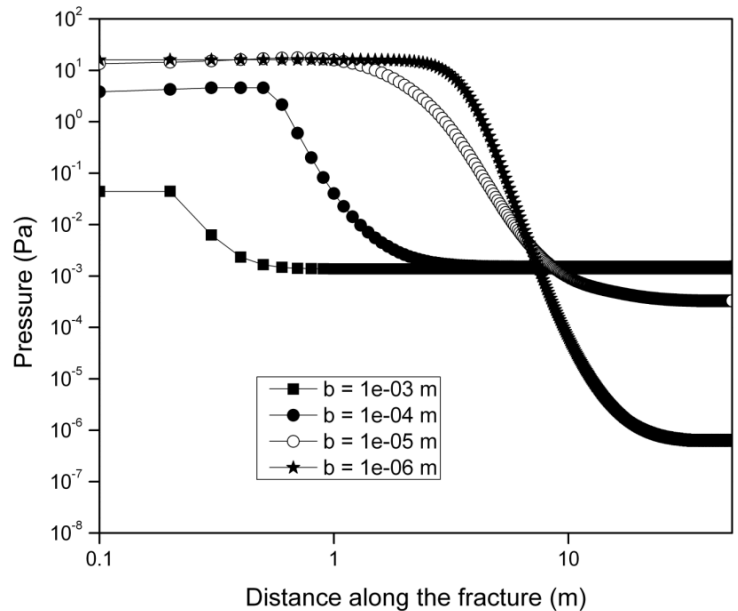


Fig. 13 Variation of pressure along the fracture for various initial half fracture apertures ($t = 5$ years, Flow rate = 5×10^{-4} $m^3/year$, fluid entering the fracture is under-saturated (100ppm), Refer Table 1 and 2 for other data)

Figure 13 shows the pressure variation along the fracture for various initial half fracture apertures. It is observed from Figure 13 that the pressure drop is very low near the injection well for large initial fracture apertures as the fracture variation is also low (Figure 12). On the other hand, for very low initial fracture apertures, pressure drops by several orders of magnitude near the injection well as the half fracture aperture also varies significantly along the fracture. The pressure remains constant close to the injection well for fracture apertures with a few microns as the aperture variation also remains constant near the injection well as observed in Figure 12.

V. CONCLUSION

The change in fracture aperture due to the heat induced thermoelastic stress and silica water interaction has been investigated in the coupled fracture-skin-matrix system in the presence of colloid transport by coupling the quartz dissolution/deposition model with that of the heat transfer model that considers the effect of thermoelastic stresses. The heat transfer between the fracture and the fracture-skin was modeled using the lateral conduction heat flux from the fracture-skin to the fracture, while the heat transport in the fracture was modeled by considering thermal advection,

dispersion and conduction. The thermoelastic stress has been computed using the analytical solution for simplicity. The pressure was allowed to vary while the discharge was assumed to remain constant along the fracture. A series of numerical simulations were carried out for examining the temporal variation of the fracture aperture and pressure in response to the individual and combined effects of thermal stress and dissolution/precipitation of silica.

The simulation results suggest that the presence of skin causes rapid transfer of heat between the rock-matrix and fracture. The contaminant concentration and temperature increases in the fracture with decrease in initial fracture aperture. In the absence of thermoelastic stress, for high initial fracture apertures, the aperture variation due to silica reaction is very marginal near to the injection well. For very small initial fracture apertures, the fracture permeability increases by several orders of magnitude as the temperature gradually increases along the fracture. Pressure variation is also observed nearer to the fracture inlet corresponding to the variation of the fracture aperture. The fracture permeability increases near to the injection well for both undersaturated as well as supersaturated fluid entering the fracture. The colloids filtered from the aqueous phase hinder the deposition of silica on the fracture surface. The colloids in the fracture affect both the thermal transport as well as contaminant transport mechanism. Thus, the presence of colloids plays a crucial role on the reservoir efficiency.

When only the thermoelastic effects are considered, a small section of the fracture close to the fracture inlet is influenced by thermoelastic stresses for different fluid velocities. When the velocity is low, there is significant residence time for the fluid in the fracture which enhances the thermal diffusion from the rock-matrix to the fracture through the medium of fracture-skin. Thus, aperture variation is marginal for low fluid velocities while the effect is significant when the fluid velocity is high.

Then, the combined effect of thermoelastic stress and chemical reaction are considered together on the variation of the fracture aperture and pressure with undersaturated fluid entering the fracture aperture. For large fracture apertures, the thermoelastic stresses influence the fracture permeability near to the injection well and silica reactivity influences the aperture variation away from the fracture inlet. For small initial fracture apertures, the thermoelastic stresses influence the permeability near to the fracture inlet but the combined thermal and chemical reactions influence the fracture permeability away from the inlet.

ACKNOWLEDGEMENT

The financial support of Department of Science and Technology, Ministry of Science and Technology, Government of India with Project No: CIE/07-08/141/DSTX/GSUR/530 is gratefully acknowledged.

REFERENCES

- [1] A. Abdel-Salam and C.V. Chrysikopolous, "Analytical solutions for one-dimensional colloid transport in saturated fractures", *Adv. Water Resour.*, vol. 17, pp. 283–296, 1994.
- [2] A. Abdel-Salam and C.V. Chrysikopolous, "Analysis of a model for contaminant transport in fractured media in the presence of colloids", *J. Hydrol.*, vol. 165, pp. 261–281, 1995.
- [3] R.S. Arvidson and F.T. Mackenzie, "The dolomite problem: the control of precipitation kinetics by temperature and saturation state", *American Journal of Science*, vol. 299, pp. 257–288, 1999.
- [4] I. Baek and W.W. Pitt, "Colloid-facilitated radionuclide transport in fractured porous rock", *Waste Management*, vol.16, pp. 313–325, 1996.
- [5] W.L. Bourcier, M. Lin, G. Nix, "Recovery of minerals and metals from geothermal fluids", SME Annual meeting, Lawrence Livermore National Laboratory, 2005.
- [6] D.R. Champ, J.L. Young, D.E. Robertson, K.H. Abel, "Chemical speciation of longlived radionuclides in a shallow groundwater flow system", *Water Pollution Research Journal Can.*, vol. 19, pp. 35–54, 1984.
- [7] C.V. Chrysikopolous and A. Abdel-Salam, "Modeling colloid transport and deposition in saturated fractures", *Colloids Surf. A: Physicochem. Eng. Aspects*, vol. 121, pp. 189–202, 1997.
- [8] J.S. Cline, R.J. Bodnar, D. Rimstidt, "Numerical simulation of fluid flow and silica transport and deposition in boiling hydrothermal solutions: applications to epithermal gold deposits", *J. Geophys. Res.*, vol. 97 (B6), pp. 9085–9103, 1992.
- [9] S.G. Driese, L.D. McKay, C.P. Penfield, "Lithologic and pedogenic influences on porosity distribution and groundwater flow in fractured sedimentary saporolite: a new application of environmental sedimentology", *Journal of Sedimentology Research*, vol. 71(5), pp. 843–857, 2001.
- [10] G.G. Eichholz, B.G. Wahlig, G.F. Powell, T.F. Craft, "Subsurface migration of radioactive waste materials by particulate transport", *Nucl. Technol.*, vol. 58, pp.511–520, 1982.
- [11] L. Fu, K.L. Milliken, J. M. Sharp Jr, "Porosity and permeability variations in fractured and liesegang-banded Breathir sandstones(middle Pennsylvanian), eastern Kentucky : diagenetic controls and implications for modeling dual-porosity systems", *Journal of Hydrology*, vol. 154, pp. 351–381, 1993.

- [12] A. Ghassemi and G. Suresh Kumar, "Changes in fracture aperture and fluid pressure due to thermal stress and silica dissolution/precipitation induced by heat extraction from subsurface rocks", *Geothermics*, vol. 36, pp. 115-140, 2007.
- [13] M.B. Hesham, A.E. Hassan, R.H. Burr, C. Papelis, "Experimental and Numerical Investigations of Effects of Silica Colloids on Transport of Strontium in Saturated Sand Columns", *Environmental Science and Technology*, vol. 40(17), pp. 5402-5408, 2006.
- [14] M. Ibraki and E.A. Sudicky, "Colloid facilitated contaminant transport in discretely fractured porous media-I Numerical formulation and sensitivity analysis", *Water Resources Research*, vol. 31, pp. 2945-2960, 1995.
- [15] R. Kretzschmar, M. Borkovec, D. Grolimund, M. Elimelech, "Mobile subsurface colloids and their role in contaminant transport", *Adv. Agron.*, vol. 66, pp. 121-194, 1999.
- [16] R.P. Lowell, P. Van Cappellen, L.N. Germanovich, "Silica precipitation in fractures and the evolution of permeability in hydrothermal upflow zones", *Science*, vol. 260, pp. 192-194, 1993.
- [17] R.C.M. Malate, M.J. O'Sullivan, "Mathematical modeling of non-isothermal silica transport and deposition in a porous medium" *Geothermics*, vol. 21, pp. 519-544, 1992.
- [18] K.S. McLin, J.N. Moore, J. Hulen, J.R. Bowman, B. Berard, "Mineral characterization of scale deposits in injection wells; Coso and Salton Sea geothermal fields", CA. Proceedings of Thirty first workshop on Geothermal reservoir engineering, Stanford University, California, 2006.
- [19] N. Natarajan and G. Suresh Kumar, "Effect of thermo and poroelasticity on the evolution of fluid permeability in a coupled fracture-skin-matrix system", Proceedings of the ninth international conference on hydro-science and engineering. August 2-5, 2010a.
- [20] N. Natarajan and G. Suresh Kumar, "Radionuclide and colloid co-transport in a coupled fracture-skin-matrix system", *Colloids Surf. A: Physicochem. Eng. Aspects*, vol. 370, pp.49-57, 2010b.
- [21] N. Natarajan and G. Suresh Kumar, "Numerical Modeling and Spatial Moment Analysis of Thermal Fronts in a Coupled Fracture-Skin-Matrix System" *Geotechnical and Geological Engineering*, vol. 29, pp. 477-491.
- [22] A. Polak, A.S. Grader, R. Wallach, R. Nativ, "Chemical diffusion between a fracture and the surrounding matrix, measurement by computed tomography and modeling", *Water Resources Research*, vol. 39(4), pp. 1106, 2003.
- [23] V.V. Potapov, G.A. Karpov, V.M. Podverbnyi, "Removal of Silica from geothermal brine" *Theoretical foundations of chemical engineering*, vol. 36(6), pp. 589-595, 2002.
- [24] J. Ren and A.I. Packman, "Modelling of simultaneous exchange of colloids and sorbing contaminants between streams and streambeds", *Environmental Science and Technology*, vol. 38, pp. 2901-2911, 2004.
- [25] J.D. Rimstidt and H.L. Barnes, "The kinetics of silica-water reactions", *Geochim. Cosmochim. Acta*, vol. 44, pp. 1683-1699, 1980.
- [26] B.A. Robinson, "Quartz dissolution and silica deposition in hot dry rock geothermal systems", M.S. thesis, MIT, 1982.
- [27] N.I. Robinson, J.M. Sharp, I. Kreisel, "Contaminant transport in sets of parallel finite fractures with fracture skins", *J. Contam. Hydrol.*, vol. 31, pp. 83-109, 1998.
- [28] B.A. Robinson and J. Pendergrass, "A combined heat transfer and quartz dissolution/deposition model for a hot dry rock geothermal reservoir", Proceedings of the 14th Stanford Geothermal Workshop, Stanford University, pp. 207-212, 1989.
- [29] A. Satman, Z. Ugur, M. Onur, "The Effect of Calcite Deposition on Geothermal Well Inflow Performance", *Geothermics*, vol. 4(1), pp. 425-444, 1999.
- [30] J.M. Sharp, "Fractured aquifers/reservoirs; Approaches, problems, and opportunities. In: Banks, D., Banks, S. (Eds), *Hydrogeology of Hard Rocks*", Memoires of the 24 th Cong. International Assoc. Hydrogeologists. Oslo Norway 24 part 1, pp. 23-28, 1993.
- [31] C.I. Steefel and P.C. Lichtner, "Multicomponent reactive transport in discrete fractures. I. Controls on reaction front geometry", *Journal of Hydrology*, vol. 209, pp.186-199, 1998.
- [32] G. Suresh Kumar and A. Ghassemi, "Numerical modeling of non-isothermal quartz dissolution in a coupled fracture-matrix system", *Geothermics*, vol.34, pp.411-439, 1995.
- [33] J. Taron and D. Elsworth, "Thermal-hydrologic-mechanical-chemical processes in the evolution of engineered geothermal reservoirs", *International Journal of Rock Mechanics and Mining sciences*, vol. 46, pp. 855-864, 2009.
- [34] J. Taron, D. Elsworth, K. Min, "Numerical simulation of thermal-hydrologic-mechanical-chemical processes in deformable, fractured porous media", *International Journal of Rock Mechanics and Mining sciences*, vol.46, pp. 842-854, 2009.

[35] D.M. Thomas and J.S. Gudmundsson, "Advances in the study of solids deposition in geothermal systems", *Geothermics*, vol. 18, pp. 5-15, 1989.